Magnetic field configuration dependence of momentum transport in Heliotron J

H.Y. Lee[1], S. Kobayashi[2], M. Yokoyama[3], T. Mizuuchi[2], T. Harada[1], K. Nagasaki[2], H. Okada[2], T. Minami[2], S. Yamamoto[2], S. Murakami[4], S. Ohshima[2], L. Zang[1], Y. Nakamura[1], S. Konoshima[2], F. Sano[2]

[1]*Graduate School of Energy Science, Kyoto University, Kyoto, Japan*

[2]*Institute of Advanced Energy, Kyoto University, Kyoto, Japan*

[3]*National Institute for Fusion Science, Toki, Japan*

[4]*Graudate School of Engineering, Kyoto University, Kyoto, Japan*

1. Introduction

The driving and damping mechanism of plasma flow has been investigated in magnetically confined plasma, because it has been reported that the plasma flow is related to the radial electric field and contribute to improve the confinement in tokamaks and stellarator/heilotron devices [1,2]. The parallel magnetic field ripple causes the damping of parallel flow ($v_{||}$) due to the neoclassical (NC) parallel viscosity, which is characterized by the transit time magnetic pumping. In Compact Helical System (CHS), the effective parallel viscosity was measured experimentally and shows good agreement with the NC parallel viscosity plus the perpendicular viscosity [3]. However, to understand the effect of magnetic field configuration on the damping mechanism more precisely, it is necessary to investigate the relation between the magnetic field configuration and $v_{||}$.

In Heliotron J, which is a helical axis heliotron device, we have investigated the effect of the magnetic field configuration, such as higher magnetic Fourier component, on the damping of $v_{||}$. In this paper, the measurement of $v_{||}$ profile in three mirror configurations are reported and viscosity is discussed.

2. Experimental Setup and Results

Heliotron J is a helical-axis heliotron device with an L/M = 1/4 helical coil, where L is the pole number and M is the helical pitch of the helical coil [4,5]. In this experiment, the typical plasma parameters are as follows: plasma major radius, R = 1.2 m, averaged minor radius, a = 0.17 m, and the magnetic field strength at the magnetic axis, B_{ax} = 1.2-1.35 T. A couple of neutral beam injection (NBI) systems are equipped for plasma heating: one is co-injection and the other is counter-injection. Here, co-direction is defined as a direction of plasma current, which increases the rotational transform. The maximum acceleration voltage and the maximum port-through injection power are 30 kV and 800 kW for each beam, respectively.

The magnetic field configurations can be generated by using five types of coils, which are the helical coil, two kinds of toroidal coil (TA and TB), and two kinds of vertical coils (AV and IV).

In this paper, three mirror configurations are chosen: standard, high and reversed mirror configurations. Figure 1 shows the main magnetic Fourier components: toroidal, helical and bumpy components. The differences of toroidal and helical component are small in three mirror configurations. However, the bumpy components at ρ = 0.2 (ρ, normalized minor radius) in high, standard and reversed mirror configurations are 0.14, 0.04 and -0.02, respectively. The bumpy components increase as a function of ρ in three mirror configurations.

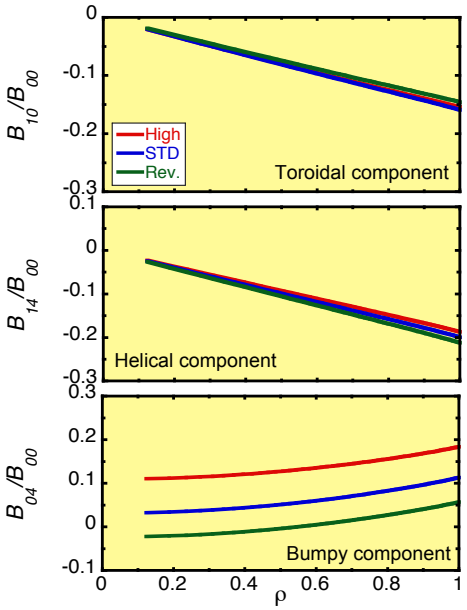

Fig.1 Main magnetic Fourier components in Heliotron J

Figure 2 shows the schematic view of CXRS system in Heliotron J. This system measures a CVI emission line (n = 7-8, 529.05 nm). As diagnostic beams, two tangential neutral beams (NBs) are used. This system has two sets of optical fiber (beam and background region) to remove cold component. These optical fibers are adopted to be symmetrical region against the toroidal direction. The number of sightline for each optical set is 14. A Czerny-Turner monochromator, whose F number is 2.8 and dispersion is 1.18 × 10^{-2} nm/pix for 529.05 nm, is installed. We mount a camera with back-illuminated CCD (ANDOR DU-887, 512 × 512 pix) on the Czerny-Turner monochromator. Line pairs (527.14 and 528.29 nm) from an Sm lamp are installed for identification of λ_0 point (529.05 nm) on the CCD images for every frame. The observable range and the radial resolution, which are estimated by a numerical calculation [6], are $0.07 < \rho < 0.94$ and $\Delta\rho \sim 0.05$ in standard mirror configuration. Details of calibration procedure for evaluating T_i and $v_{\parallel}$ are described in ref. [6].

Figure 3 shows typical time evolutions of line-averaged electron density ($\bar{n}_e$) and plasma stored energy (W_p) in three mirror configurations. The plasmas were sustained by co-NB, whose acceleration voltage was 27 kV and port-trough power was 500 kW. In these discharges, $\bar{n}_e$ were 0.8-1.0 × 10^{19} m^{-3} and W_p were 0.6-0.7 kJ in three mirror configurations. The line-averaged electron densities are almost constant after 240 ms.

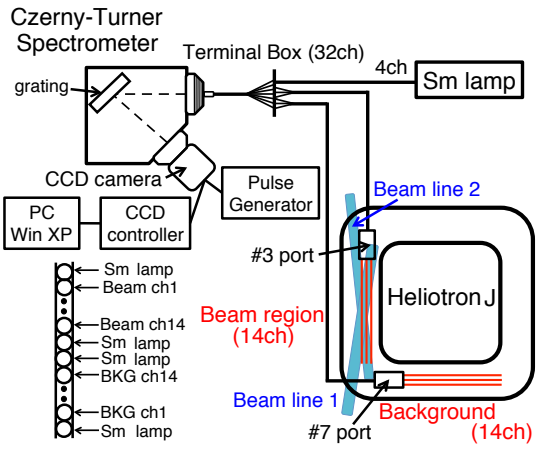

Fig.2 Schematic view of CXRS system in Heliotron J

Figure 4 shows $v_{\parallel}$ and T_i profiles measured by CXRS system in quasi-steady state (t = 247.5 ms, 252.5 ms and 242.5 ms for the high, standard and

reversed mirror configurations, respectively). The observation point and the radial resolution are estimated for each mirror configuration. The error-bars of $v_{\|}$ and T_i are estimated from the uncertainties in the Gaussian fit parameters [7]. The observation point and the radial resolution are estimated by the numerical calculation individually. We did not estimate $v_{\|}$ and T_i at $\rho > 0.8$ due to small signal-to-noise ratio. Near the plasma center (ρ = 0.07), the ion temperature in the high mirror configuration is about 20 and 40 eV higher compared to those in the standard and reversed mirror configurations, respectively. The parallel flow velocity at ρ = 0.07 in high, standard and reversed mirror configurations are 12 km/s, 10 km/s and 4 km/s, respectively. The parallel flow velocity in the high mirror configuration is 3-4 times smaller than those in standard and reversed mirror configurations.

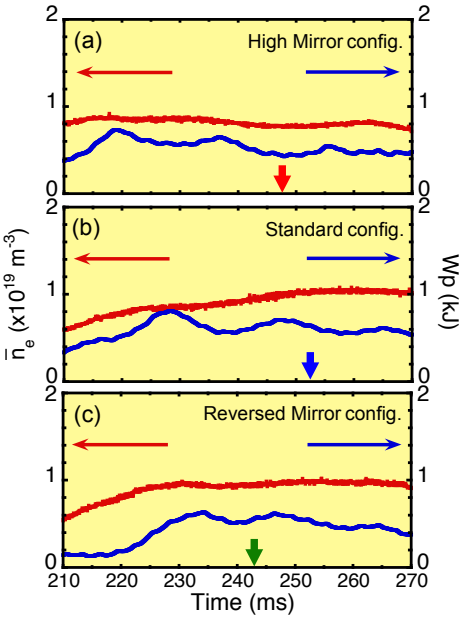

Fig.3 Time evolution of line-averaged electron density and plasma stored energy in (a) high mirror, (b) standard and (c) reversed mirror configuration.

To investigate the damping force on $v_{\|}$, we estimated the effective viscosity ($\mu_{\|\mathrm{eff}}$) with the injection power scan of NB and compared with the NC parallel viscosity. Figure 5(a) shows that $v_{\|}$ at ρ = 0.07 as a function of the external momentum input ($F_{\|\mathrm{ext}}$). The external momentum input by NBI is calculated by FIT code [8]. The electron density profile is assumed to be $n_e(\rho) = n_e(0)(1-\rho^2)$ with $n_e(0) = 1.5 \times 10^{19}$ m^{-3} and the electron temperature profile is assumed to be $T_e(\rho) = T_e(0)(1-\rho^2)$ with $T_e(0)$ = 300 eV. In this calculation, the shine-through loss, the prompt orbital loss and the charge exchange (CX) loss with thermal neutrals were included. The co-direction is defined as a positive value of $F_{\|\mathrm{ext}}$. We define $\mu_{\|\mathrm{eff}}$ near the plasma center (ρ = 0.07) as $\mu_{\|\mathrm{eff}} = \mathrm{d}F_{\|\mathrm{ext}}(0.07)/n_i m_i \mathrm{d}v_{\|}(0.07)$. The effective viscosity coefficients in high, standard and reversed mirror configurations are about 4.7×10^3 s^{-1}, 1.8×10^3 s^{-1} and 1.4×10^3 s^{-1}, respectively. On the other hand, the NC parallel viscosity coefficient in the plateau regime, which is modeled by Shaing and Callen [9], is given [9, 2] by,

$$\mu_{\|neo} \sim \xi_1 \sqrt{\pi}\gamma^2 \frac{eT_i}{m_i \omega_{ti}}, \qquad (1)$$

where, ω_{ti} is the transit frequency, m_i is the ion mass, e is

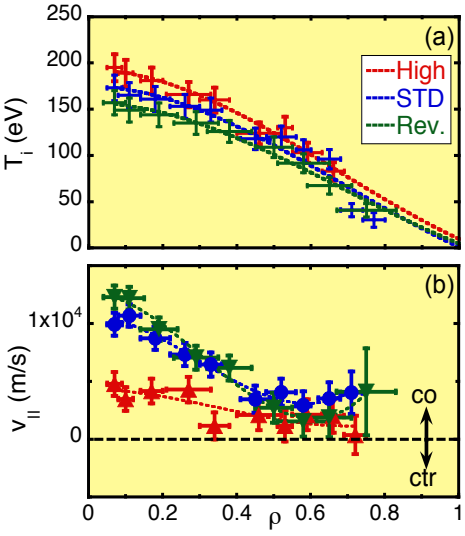

Fig.4 Radial profile of (a) ion temperature and (b) parallel flow velocity in three mirror configurations

the charge of ion, γ is the magnetic ripple strength which is defined as $\gamma^2 = <(\partial B/\partial l)^2/B^2>$. Here, l is the length along the magnetic field line. ξ_1 is the energy integral coefficient and is constant ($\xi_1 = 2$) in the plateau regime [2]. The calculated NC parallel viscosity coefficients at $\rho = 0.07$ in high, standard and reversed mirror configurations are about 1.0×10^3 s^{-1}, 0.2×10^3 s^{-1} and 0.15×10^3 s^{-1}, respectively. Figure 5(b) shows the ratio between $\mu_{\|eff}$ and $\mu_{\|neo}$ as a function of $\mu_{\|neo}$ in three mirror configurations. The effective viscosity coefficients are approximately 5-10 times larger than the NC parallel viscosity coefficients. This result suggests that the perpendicular viscosity due to the momentum diffusion should be taken into account.

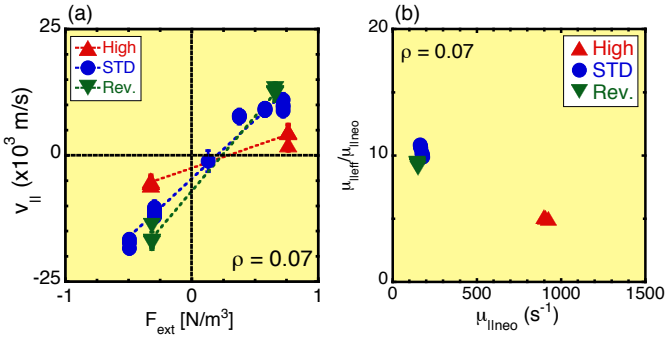

Fig.5 (a) Parallel flow velocity as a function of external momentum input and (b) ratio between $\mu_{\|eff}$ and $\mu_{\|neo}$ as a function of $\mu_{\|eff}$.

3. Summary

To investigate the effect of magnetic field configuration on the damping of $v_{\|}$, $v_{\|}$ is measured via the CXRS system in three mirror configurations. The mirror magnetic field configurations are varied by changing bumpy component. Near the plasma center ($\rho = 0.07$), the parallel flow velocity in the high mirror configuration is 3-4 times smaller than those in the standard and reversed mirror configurations. The effective viscosity coefficients are evaluated from the measured $v_{\|}$ do not agree with the NC parallel viscosity coefficients in three mirror configurations.

Acknowledgments

Authors are grateful for the great support of the Heliotron J technical staff. This work was partially supported by NIFS collaborative research program (NIF10KUHLLL030, NIFS09KUHL025) and the GCOE program in Kyoto University.

References

[1] J.S. deGrassie, Plasma Phys. and Control. Fusion, **51** (2009) 124047.
[2] K. Ida, Plasma Phys. and Control. Fusion, **40** (1998) 1429.
[3] K. Ida *et al*., Phys. Rev. Lett., **67** (1991) 58.
[4] M. Wakatani *et al*., Nucl. Fusion **40**, (2000) 569.
[5] M. Yokoyama *et al*., Nucl. Fusion **40**, (2000) 261.
[6] H.Y. Lee, Plasma and Fusion Research, **7** (2012) 1402019.
[7] K. H. Burrell *et al*., Am. J. Phys., **58**, (1990) 2.
[8] S. Murakami *et al*., Trans. Fusion Tech. **27,** 259 (1995).
[9] K. C. Shaing and J. D. Callen, Phys. Fluids, **26** (1983) 1526.